0026-895X/96/030430-08$3.00/0

MOLECULAR PHARMACOLOGY, 49:430–437 (1996).

Variants of Human Dihydrofolate Reductase with Substitutions at Leucine-22: Effect on Catalytic and Inhibitor Binding Properties

EMINE A. ERCIKAN-ABALI, MARK C. WALTHAM, ADAM P. DICKER, BARRY I. SCHWEITZER, HELENA GRITSMAN, DEBABRATA BANERJEE, and JOSEPH R. BERTINO

Program of Molecular Pharmacology and Therapeutics, Memorial Sloan-Kettering Cancer Center, New York, New York 10021 (M.C.W., A.P.D., B.I.S., H.G., D.B., J.R.B.), and Graduate School of Medical Sciences, Cornell University, New York, NY 10021 (E.A.E.-A.)

Received March 24, 1995; Accepted November 7, 1995

SUMMARY

We investigated the enzyme kinetic and antifolate inhibitory properties of human dihydrofolate reductase enzyme with mutations at position 22. Leu-22 was changed to isoleucine, methionine, phenylalanine, and tyrosine to generate the various mutant enzymes. The overall catalytic efficiency (k_{cat}/K_m) for methionine and phenylalanine mutants was reduced ~3-fold and >6-fold for isoleucine and tyrosine mutants. An arginine mutant ($L^{22}R$) was also expressed but had a dramatically reduced catalytic potential (k_{cat} >250-fold lower than wild-type) and therefore was not studied in detail. The K_i for antifolates, methotrexate, aminopterin, and trimetrexate are more dramatically affected (increased) than the K_m for dihydrofolate, particularly for phenylalanine and tyrosine mutants. One remarkable feature is that the phenylalanine mutant is as potently inhibited by piritrexim as is the wild-type human enzyme, although the K_i values for methotrexate and aminopterin were increased 88- and 118-fold, respectively. This is likely related to different positioning of the methoxyphenyl side chain of piritrexim relative to the side chains of other compounds tested. A Chinese hamster cell line harboring the $L^{22}F$ mutant also demonstrated an increased sensitivity to piritrexim relative to antifolates.

One mechanism of MTX-resistance observed in cultured tumor cell lines (1–6) and in an experimental mouse model (7) has been mutations in the DHFR gene, which result in altered DHFRs with reduced antifolate binding ability. An $L^{22}F$ mutation in DHFR (4) has been identified from the MTX-resistant CHO cell line $Pro^{-}3$ Mtx^{RIII} (8, 9). Kinetic studies of the altered enzyme revealed that the K_m for both substrates (7,8-dihydrofolate and NADPH) were similar when compared with the WT vertebrate enzyme, but the K_i for MTX was increased ~100-fold. Moreover, in previous studies by others mutations at codon 22 were also identified in MTX-resistant murine cell lines: a leucine-to-arginine mutation in 3T6-R400 (2) and a leucine-to-phenylalanine mutation in another CHO cell line (3). In these or subsequent studies, a reduced MTX binding for the altered enzyme was confirmed. Codon 22 (L) (2–6) appears to be "hot spot" for mutations in the eukaryotic DHFR gene, giving rise to mutations that decrease binding of antifolates to the enzyme.

These findings indicated that substitutions at residue 22 of human DHFR reduce the binding of antifolates with less effect on the binding of substrates for DHFR. Moreover, it seems plausible that these or similar mutations in DHFR are responsible for some instances of resistance in tumors of patients who receive antifolates therapeutically, although there is no definitive proof of this.

MTX-resistant mutants of DHFR are of current interest for use as amplifiable-dominant selectable markers in gene transfer and as part of a therapeutic means to render antifolate resistance to bone marrow stem cells. The introduction of drug resistance genes into marrow progenitor cells has been proposed as a method for permitting larger doses of the relevant drug in subsequent therapy (i.e., less toxicity) (10). Several recent murine studies (11, 12) have confirmed that marrow tolerance to MTX is improved after the gene encoding for a mutant murine DHFR is transfected into marrow progenitor cells (13). It may also be possible to cotransfect other nonselectable desired genes (e.g., adenosine deaminase) along with a variant of DHFR with the use of retroviral vectors, followed by treatment with low, nontoxic doses of MTX to select for stem cells containing these transfected genes. It is important to characterize mutant human DHFR

This work was supported by United States Public Health Service Grant CA08010. J.R.B. is an American Cancer Society Professor. E.A.E-A. and M.C.W contributed equally to this work.

ABBREVIATIONS: DHFR, dihydrofolate reductase; WT, wild-type; BSA, bovine serum albumin; CHO, Chinese hamster ovary; MTX, methotrexate; APT, aminopterin; TMTX, trimetrexate; PTX, piritrexim; PCR, polymerase chain reaction; MES, 2-(*N*-morpholino)ethanesulfonic acid; MATS, 2-(*N*-mopholino)ethanesulfonic acid/acetic acid/Tris base/sodium chloride buffer.

genes rather than murine genes in view of the potential applications.

We report the characterization of variants of human DHFR with substitutions at Leu-22. Molecular modeling studies enabled predictions to be made regarding substrate and antifolate binding for different possible side-chain replacements. Proteins with substitutions of isoleucine, methionine, phenylalanine, tyrosine, and arginine were recombinantly expressed to determine the changes on the properties of substrate and antifolate binding of the mutant human enzymes. Correlations between experimental data and predictions are discussed as well as the suitability of these mutants for use in gene transfer.

Experimental Procedures

Materials. *Taq* DNA polymerase and restriction enzymes were obtained from Boehringer Mannheim (Indianapolis, IN). DEAE-Sephacel and dNTP were obtained from Pharmacia (Piscataway, NJ), ultrafiltration materials were obtained from Amicon (Lexington, MA), and DNA purification was done with the GeneClean Kit from Bio 101 (Vista, CA). Sequencing was carried out with Sequenase Version 2.0 from United States Biochemical Corp. (Cleveland, OH). Isopropyl β-D-thiogalactopyranoside was also purchased from United States Biochemical Corp., and ampicillin was obtained from from International Biotechnologies (New Haven, CT). DNase I, leupeptin, lysozyme, folic acid, NADPH, and BSA were from Sigma Chemical Co. (St. Louis, MO). Bacterial growth and tissue culture media were obtained from an in-house media unit. Fetal bovine serum, L-glutamine, penicillin, streptomycin, and molecular weight standards were from GIBCO-BRL (Gaithersburg, MD).

Inhibitor compounds were obtained from different sources: MTX, Lederle Labs. (Pearle River, NY); TMTX, Parke-Davis Clinical Research (Warner-Lambert Co., Ann Arbor, MI); APT, Sigma Chemical Co.; and PTX, Burroughs Wellcome Co. (Research Triangle Park, NC). The concentrations of ligands were determined spectrophotometrically. All other reagents were high-purity preparations from commercial sources or as previously specified (14).

Mutagenesis of human DHFR. Mutagenesis (excluding that for the $L^{22}R$ construct) was performed with a PCR technique that involved two separate sets of primers (Table 1): one set flanks the entire cDNA of DHFR, and the second set is complementary to the other and contains the desired mutation (15). For $L^{22}R$, a one-step PCR procedure was used with the mutant primer (90 mer; Table 1) annealing coding strand and the second primer binding the noncoding strand to produce the entire, desired cDNA. The final PCR products (incorporating a mutated full-length cDNA) were digested with *Nco*I and *Hin*dIII and cloned into a pKT7 expression vector (14) containing the same restriction sites. The resulting ligation mixtures were used to transform *Escherichia coli* BL21 (DE3).

The complete cDNA of the different mutant enzyme species contained in the expression vector was sequenced (16) with six different oligonucleotides: three were complementary to the 3′-noncoding strand, and the other three were complementary to the 5′-coding strand. No additional (unintended) base mutations were found.

TABLE 1

Oligonucleotides used for PCR mutagenesis

Created mutation	
$L^{22}I$	5′ CCA GGG AAT GTC CCC GTT 3′
	3′ GGT CCC TTA CAG GGG CAA 5′
$L^{22}M$	5′ CCA GGG ATG GTC CCC GTT 3′
	3′ GGT CCC TAC CAG GGG CAA 5′
$L^{22}F$	5′ CCA GGG TTT GTC CCC GTT 3′
	3′ GGT CCC AAA CAG GGG CAA 5′
$L^{22}Y$	5′ TGG CCA GGG TAC GTC CCC GTT CTT 3′
	3′ ACC GGT CCC ATG CAG GGG CAA GAA 5′
$L^{22}R$[a]	5′ ----------CGG----------3′

[a] Mutagenesis by one-step PCR as detailed in Experimental Procedures.

Expression of recombinant mutant human DHFR and preparation of crude bacterial lysate. Small overnight growths of BL21 containing the expression plasmids were used to inoculate 1–3 liters of 2× tryptone/yeast medium (16 g/liter tryptone, 10 g/liter yeast extract, 5 g/liter NaCl) containing 200 μg/ml ampicillin. Bacteria were grown to an A_{600} of 1.0. Isopropyl β-D-thiogalactopyranoside was then added to achieve a final concentration of 2 mM and to initiate synthesis of the human enzyme. After 4–6 hr, bacteria were harvested by centrifugation at 4°, washed in M9 salt solution, and then resuspended in 10–30 ml of cold lysis buffer (50 mM Tris·HCl, pH 7.0, 100 mM KCl, 10% glycerol, 2 mM dithiothreitol, 1 mM PMSF, 1 μg/ml leupeptin, 1 mM EDTA). Lysozyme was added (0.3 mg/ml), and the solution kept on ice for 30 min. DNase (0.1 mg/ml) and $MgCl_2$ (5 mM) were added, and the viscous suspensions were maintained on ice for an additional 30 min. Mixtures were then sonicated with six 20-sec bursts with a Vibracell sonicator (Sonics and Materials, Danbury, CT), followed by centrifugation at 100,000 × *g* for 30 min. Supernatants were either snap-frozen in liquid nitrogen and stored (−75°) or used directly in purification.

Activity and stability of mutants. Preliminary experiments with small-scale growths of bacteria and following the extraction procedures outlined above indicated that maximal expression of enzyme (on the basis of specific activity) was 4–6 hr for each mutant. Activity was determined with a spectrophotometric procedure where conversion of NADPH and 7,8-dihydrofolate to $NADP^+$ and 5,6,7,8-tetrahydrofolate is followed at 340 nm (17). The routine assay conditions included MATS assay buffer (25 mM MES, 25 mM acetic acid, 50 mM Tris base, 100 mM sodium chloride) (18), pH 7.4, supplemented with 50 μg/ml BSA, 1 mM dithiothreitol, and 50 mM β-mercaptoethanol, and substrate (H_2,folate) and cofactor (NADPH) at final concentrations of 50 μM and 100 μM, respectively. The stability of recombinant enzyme in crude bacterial lysates was assessed by diluting extract in lysis buffer to 1 mg/ml (total protein concentration) and then assaying activity periodically at 25° (Fig. 1a).

Levels of activity for crude extracts were correlated with the intensity (laser densitometry) of the 22-kDa DHFR protein band after sodium dodecyl sulfate-polyacrylamide gel electrophoresis and Coomassie blue staining. The activity of the $L^{22}R$-containing cytosols was particularly low yet contained considerable amount of expressed 22-kDa protein, as shown in Fig. 1b.

Purification of mutant dihydrofolate reductase. As it was anticipated that mutant species may bind less tightly to MTX, we modified a traditional (19) MTX affinity chromatography purification step for WT DHFR as outlined in other reports from this laboratory (7); only $L^{22}R$ was not purified. Fractions containing activity after 7,8-dihydrofolate absorption from the resin were directly dialyzed against 50 mM Tris·HCl, pH 7.2, and then concentrated on YM10 membranes (Centriprep 10 units, Amicon). Residual 7,8-dihydrofolate and contaminating proteins were removed by passage on DEAE-Sephacel columns pre-equilibrated with 10 mM Tris, pH 7.2, 1 mM EDTA, and 100–500 mM NaCl elution gradient. A preparation of crude, recombinant WT human DHFR was purified in an identical manner next to mutant species. Enzyme purity was evaluated by sodium dodecyl sulfate-polyacrylamide gel electrophoresis and specific activity measurements. Protein was determined according to the method of Bradford (20).

Enzyme characterization. Enzyme kinetic studies were performed at 24° with the MATS assay buffer system (19), pH 7.4, containing BSA and thiol additives as previously mentioned, and with a Shimadzu UV-2101 PC spectrophotometer. Some pH-dependency studies also used the MES/Tris base/Ethanolamine/NaCl buffer system (25 mM MES, 25 mM Tris base, 25 mM ethanolamine, 100 mM NaCl) (18). $L^{22}R$ DHFR was not studied.

K_m values for 7,8-dihydrofolate were determined from initial velocity measurements of DHFR at variable concentrations of 7,8-dihydrofolate and a saturating level of cofactor NADPH (50 μM).

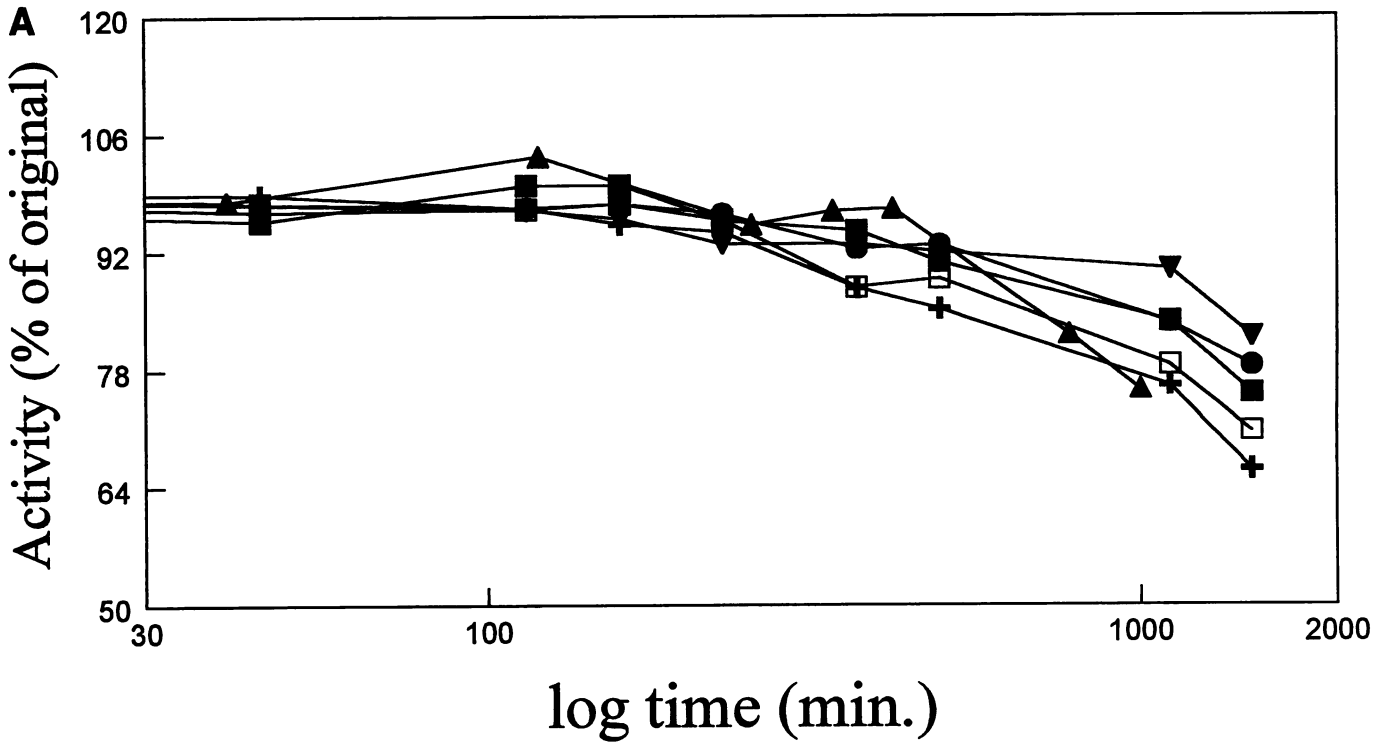

Fig. 1. Expression and stability of human dihydrofolate reductase mutants in host lysates. A, The content of recombinantly expressed protein in *BL21* cytosols was assessed by sodium dodecyl sulfate-polyacrylamide gel electrophoresis followed by Coomassie blue staining. Protein (30 μg) was loaded for extracts at the growth time point of maximal specific activity. +, WT; ■, $L^{22}I$; ▼, $L^{22}M$; □, $L^{22}F$; ●, $L^{22}Y$; ▲, $L^{22}R$. B, Time course stability analysis of WT and mutant DHFRs in crude *BL21* cytosols. Extracts (including three non-residue-22 mutants) were diluted to a uniform total protein concentration and maintained at 25°, and portions were assayed periodically for remaining activity. *Lane 1*, $L^{22}R$; *lane 2*, *E. coli* host (no expression plasmid); *lane 3*, $L^{22}Y$;*lane 4*, $L^{22}F$; *lane 5*, WT.

Cuvette cells (10-cm pathlength) were used to monitor slow reaction rates at low 7,8-dihydrofolate concentrations. Parameter values were subsequently determined by fitting data to the Michaelis-Menten equation using nonlinear, least-squares regression analysis (21). As an inhibition phenomena at "high" 7,8-dihydrofolate concentrations was observed, only data obtained at lower (subinhibitory) concentrations were used in the evaluation of K_m for this substrate.

Enzyme active site concentration (and thus total enzyme concentration) for the purified WT and mutant human DHFR preparations was determined by titrating enzyme activity with MTX (22).

K_i values were obtained from steady state inhibition reaction rates for mixtures of enzyme, cofactor, substrate, and inhibitor. Multiple assays (>10) were performed at a fixed (high) 7,8-dihydrofolate concentration (150 μM) and variable antifolate concentrations for any one data set. In many instances, reactions were monitored for >1 hr due to the slow binding of drugs under these particular conditions. A competitive (tight-binding) mode of inhibition was assumed, and the corresponding equations (21, 23) were used to fit (22) to data. These equations reduce to the classic equation for competitive inhibition under conditions where free inhibitor concentration is not significantly depleted when it complexes with enzyme. It is therefore also appropriate for the analysis of data from mutants with greatly reduced inhibitor binding.

Cell culture conditions and antifolate sensitivity. The CHO cell line Pro^{-3} ("parental") and the MTX-resistant subline Pro^{-3} Mtx^{RIII} (8, 9) were kindly supplied by Dr. W. Flintoff (University of Western Ontario, London, Ontario, Canada) and Dr. L. Chasin (Columbia University, New York, NY). Stock cultures of both lines were maintained as monolayers in RPMI 1640 medium supplemented with 10% fetal calf serum, 2 mM L-glutamine, 100 μg/ml streptomycin, and 100 units/ml penicillin.

Sensitivity to antifolates was determined by first plating ~200 cells of each cell line (each in exponential growth phase) into 34-mm culture plates. On the following day, media were removed from adhered cells and replaced with fresh media (5 ml) containing MTX, TMTX, APT, and PTX at one of nine different concentrations ranging

TABLE 2

Steady state kinetic properties of WT and residue 22 mutants of DHFR

The spectrophotometric assay and MATS buffer (pH 7.4, 24°) were used in all determinations. Michaelis constants (for H_2 folate) were evaluated by fitting the hyperbolic form of the Michaelis-Menten equation (iterative analysis) to initial velocity measurements. Cuvettes with 10-cm pathlengths were used in these instances to assist in monitoring reactions at low H_2 folate concentrations. Values of k_{cat} were obtained by active site titration (1-cm pathlength cuvettes) with MTX^{22} and/or from activity and total protein measurements of purified enzyme. Standard errors for estimates are <10%.

	WT	$L^{22}I$	$L^{22}M$	$L^{22}F$	$L^{22}Y$	$L^{22}R^a$
K_m (μM)	0.08	0.55	0.23	0.16	0.15	n.d.
k_{cat} (sec^{-1})	12.7	13.2	13.4	7.4	1.5	< .05
k_{cat}/K_m (sec^{-1} μM^{-1})	159	24	58	46	10	

[a] k_{cat} for $L^{22}R$ was determined from activity measurements of crude extract and an estimate of enzyme protein (i.e., 22-kDa portion) on SDS-PAGE.
n.d. = not determined.

from 1 nM to 10 μM (each concentration in duplicate). Fresh media containing drug were replaced after 1 week; then, colonies were maintained for an additional week before fixing (0.4% formaldehyde) and staining with crystal violet. Colonies containing ≥50 cells were scored and compared with triplicate, untreated controls that were maintained under identical conditions. Linearized plots of cell survival as a function of antifolate concentration were used to derive IC_{50} and IC_{90} values for colony survival. These values represent the drug concentrations corresponding to 50% and 90% suppression in colony numbers, respectively.

Protein structure modeling. All eukaryotic species of this enzyme display a high degree of structural homology, particularly at the active site region. In the absence of human DHFR crystal coordinate data, we have used the chicken DHFR/NADPH atomic crystal coordinate complex (24) as a basis to construct a three-dimensional model of the human DHFR active site (14). MTX was modeled into the active site structure by determining the optimal rotation/translation matrix to best superimpose key active site atoms of the the human model. Folate was modeled into the active site by superimposition onto MTX with the pteridine moiety in the twisted/inverted orientation (24, 25). With the availability of the human DHFR crystal data, we were able to validate that the active site of the model we had constructed was identical to the human DHFR active site. Models were displayed on a silicon graphics personal Iris using the Polygen Quanta software.

Results

Enzyme kinetic properties. Steady state enzyme kinetic properties for the WT and mutant DHFRs (excluding $L^{22}R$) were evaluated to probe the catalytic role of the Leu-22 residue and the catalytic properties of the altered enzyme (Table 2). Cofactor binding was not assessed. All mutants displayed an increased K_m for 7,8-dihydrofolate; the more conserved replacements (M and I) resulted in a 6-fold increase in K_m, whereas the bulkier side-chain replacements (F and Y) displayed only ~2-fold increase in K_m. In contrast, the maximal catalytic turnovers (k_{cat}) for purified $L^{22}F$ and $L^{22}Y$ enzymes are more affected than $L^{22}I$ and $L^{22}M$, with the latter essentially identical to WT enzyme (Table 2).

During catalytic cycling of DHFR, an increase in the relative [$NADP^+$]/[NADPH] ratio (indicating accumulation of $NADP^+$) results in a progressive decrease in reaction rate. This phenomenon has been ascribed to the enzyme channeling through one of the alternative, slower catalytic routes as defined by Blakley *et al.* (26) and is readily observed with the spectrophotometric assay. To assess the propensity for this "product inhibition," complete progress curves for catalysis by the different DHFR species were examined under the appropriate conditions (see Experimental Procedures) of limiting and nonlimiting cofactor concentration. The resulting progress curves for WT were similar to those reported earlier

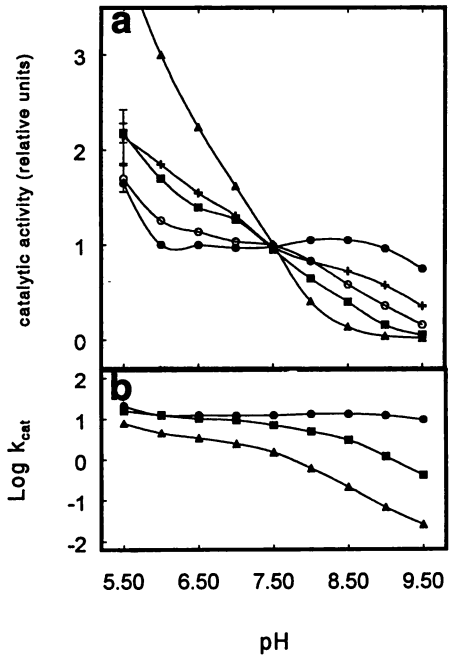

Fig. 2. pH rate profiles for WT and residue-22 mutants of dihydrofolate reductase. Assays were performed in MES/Tris base/Ethanolamine/NaCl buffer at 24°. ●, WT; ○, $L^{22}I$; +, $L^{22}M$; ■, $L^{22}F$; ▲, $L^{22}Y$. a, Rates normalized for activity at pH 7.4 (i.e., rate at pH 7.4 set to 100). b, pH versus log k_{cat} for selected species.

(26) and essentially identical to those for each of the four mutant species studied in detail (data not presented). However, all species, including WT, displayed distinct inhibition of initial velocities when 7,8-dihydrofolate concentrations exceeded 5–10 μM (depending on species), regardless of cofactor concentration; this is consistent with our previous observations.[1] We would like to note that the different k_{cat} and K_m values obtained for certain human DHFR mutants by Nakano *et al.* (27) and by our laboratory were not due to differences in the method of analysis (i.e., taking into account substrate/product inhibition) but rather to a difference in pH at which the kinetic data were obtained. We therefore did not obtain evidence for an altered catalytic pathway for any of the position 22 mutants (under the standard assay conditions), although clearly the experimental approach adopted here is only qualitative in this respect.

The variation of catalytic activity with pH for the different species of DHFR is depicted in Fig. 2a. The profile for WT is relatively flat except for the extreme acidic region examined

[1] M. C. Waltham and J. R. Bertino, manuscript in preparation. The manuscript includes an analysis of the effect when determining kinetic and inhibition parameters.

(pH 5.5–6.0). All mutants examined displayed a degree of pH dependency with lower rates at higher pH. The $L^{22}Y$ mutant shows marked pH dependency with a catalytic rate 2.2-fold higher at pH 6.5 and 5.5-fold higher (Fig. 2a, *off scale*) at pH 5.5. A pH-log k_{cat} plot (Fig. 2b) reveals complete pH dependency for this mutant (slope of −1) across the entire pH range. $L^{22}F$ also displays essentially complete pH dependency but only at ≥pH 8.5. pH at which catalytic rate is equally limited by product dissociation (pH independent) and hydride transfer (pH dependent) is ~7.5 for $L^{22}Y$, ~8.1 for $L^{22}F$, and considerably higher for other mutants and WT.

Affinity for antifolate compounds. The inhibition constants for WT and mutant DHFRs, for classic antifolate compounds (MTX and APT), and for the newer, lipophilic compounds (TMTX and PTX) are presented in Table 3. The binding affinity of MTX for $L^{22}F$ is significantly reduced (88-fold), which is consistent with data obtained for the hamster version of this mutant (4) and consistent with what may be anticipated for a mutant providing MTX resistance in cultured cell lines. APT also binds less tightly (118-fold) for this mutant. $L^{22}Y$ binds MTX and APT least tightly of all mutants. Mutations with more conserved residue replacements display only marginally reduced binding for these classic antifolates.

The most surprising finding for this series of compounds examined is that PTX binds with almost identical strength to $L^{22}F$ as it does to WT (Table 3). In contrast, the other lipophilic drug, TMTX, has 6.5-fold reduced binding, and $L^{22}Y$ has greatly reduced binding for both PTX and TMTX.

Progress curves from inhibition studies of WT displayed the phenomena of "slow tight binding" under the specified reaction conditions and for all compounds studied (not depicted). This is attributed to a slow isomerization of an initial ternary complex (enzyme/NADPH/antifolate) to form a final, pseudoirreversible complex (22) and has been observed for all WT species of DHFR under standard assay conditions, at least when undergoing inhibition by MTX. A similar slow progress of inhibition was identified for $L^{22}I$ and $L^{22}M$ in combination with antifolates (Table 3) yet was absent for $L^{22}Y$ with each of the four antifolates. This undoubtedly accounts, in part, for the lower overall binding affinity of these compounds to the tyrosine mutant (i.e., higher K_i values). For $L^{22}F$, an isomerization process in progress curves was barely discernible for MTX, APT, and TMTX, although apparent when in combination with PTX. For this mutant, the final steady state rates were only slightly slower than initial inhibited reaction rates.

Cell culture cytotoxicity studies. The series of antifolate compounds examined in enzyme kinetic studies were also assessed in their cytotoxicity toward two CHO cell lines: (i) the CHO $Pro^{-}3$ parental line, which is sensitive to MTX and expresses WT (CHO) DHFR, and (ii) the CHO $Pro^{-}3$ Mtx^{RIII} line, which is MTX resistant and expresses increased amounts of $L^{22}F$ (CHO) mutant DHFR (4, 28). A procedure that quantifies colony survival after a 14-day exposure to each drug was used. Data are presented in Table 4.

Parental cells are sensitive to all antifolates examined, with IC_{50} and IC_{90} values within the nanomolar range. APT is the most cytotoxic agent for this line, being more potent than MTX, which is a finding common for cultured cell lines. The $Pro^{-}3$ Mtx^{RIII} line displays considerable resistance to MTX, with IC_{50} and IC_{90} values 42- and 177-fold greater, respectively, than parental cells. Of significance is the greater cytotoxicity of PTX toward $Pro^{-}3$ Mtx^{RIII} in comparison to MTX: 10.5-fold lower and 50-fold lower for IC_{50} and IC_{90} respectively. Sensitivity of $Pro^{-}3$ Mtx^{RIII} toward the other lipophilic antifolate investigated (TMTX) is less marked. Moreover, examination of the ratio of cytotoxicity evaluated for each cell line (i.e.,. $Pro^{-}3$ Mtx^{RIII}/parental) and for each drug (Table 4) highlights the greater sensitivity to PTX for the line harboring the mutant DHFR.

Discussion

To understand attenuations in binding of ligands with position 22 residue replacements, we undertook computer modeling of the human DHFR site incorporating folic acid, cofactor (NADPH), and inhibitor. From studies of the crystal structure on DHFR (24, 29) the active site Leu-22 is in close proximity and contributes hydrophobic interactions with folate. Two possible consequences could be anticipated with respect to substrate binding: one is a loss of binding energy due to the loss of hydrophobic interaction, and the other is a steric disruption of ligand binding for amino acid replacements with large side-chain volume. On this basis, the more conserved replacements $L^{22}M$ and $L^{22}I$ should show little reduction in 7,8-dihydrofolate affinity (i.e., minimal increase in K_m), whereas $L^{22}Y$ should show the greatest. On the other hand, the distance between the two closest atoms of either Leu-22, Phe-22, or Tyr-22 and NADPH is not significantly altered (3.64, 3.73, and 3.73 Å, respectively) and therefore should not directly alter cofactor affinity. The effect on binding of MTX was expected to be much greater. One view of the spatial orientation of residue 22 with MTX and folate is given in Fig. 3a. As depicted, MTX binds in a flipped orientation, with the pteridine rotated 180° about the C_6—C_9 bond axis (relative to the pteridine ring of folate) (24, 25). A consequence of this is that the bridge region between the pteridine

TABLE 3

Inhibition constants for WT and residue 22 mutants of DHFR

The spectrophotometric assay and MATS buffer (pH 7.4, 24°) were used in all determinations. Values were obtained by fitting the equation for tight-binding competitive inhibition to inhibited steady state data, so a competitive mode of interaction (with respect to 7,8-dihydrofolate) was assumed. Initial 7,8-dihydrofolate and NADPH concentrations in assays were 150 and 200 μM, respectively. Standard errors for all estimates are <15%.

	WT	$L^{22}I$	$L^{22}M$	$L^{22}F$	$L^{22}Y$
			pM		
MTX	1.2	1.8	2.8	106	1980
APT	1.8	7.2	9.2	212	1277
TMTX	13.0	n.d.	n.d.	83.3	2514
PTX	13.2	n.d.	n.d.	16.0	1190

[a] Values determined previously in this laboratory under similar experimental conditions.
n.d. = not determined.

TABLE 4

Clonogenic cytotoxicity of CHO Pro$^-$3 (parental) and CHO Pro$^-$3 Mtx^{RIII} (MTX-resistant) cells by antifolates

Plated cells were exposed to a range of drug concentrations (no antifolate and 1 nM-10 μM) for 14 days; then, surviving colonies visually scored after fixing and crystal violet staining. Further details are provided in Experimental Procedures. IC_{50} and IC_{90} (averages from duplicate determinations) represent the drug concentrations that suppress colony numbers by 50% and 90%, respectively.

	IC_{50}			IC_{90}		
	Pro$^-$3	Pro$^-$3 Mtx^{RIII}	Ratio	Pro$^-$3	Pro$^-$3 Mtx^{RIII}	Ratio
	nM	nM		nM	nM	
MTX	7	295	42	30	3500	117
APT	1	35	35	3	325	108
TMTX	4	130	32	17	310	18
PTX	5	28	6	8	67	8

[a] Resistance ratio for CHO Pro$^-$3 Mtx^{RIII} to Pro$^-$3.

and *p*-aminobenzoyl moiety (see Fig. 3b), which includes the methyl group of N_{10}, is oriented closer to the 22 position. The distance between the N_{10} and Leu-22 of WT is ~5 Å, whereas the corresponding distance to the closest carbon of a phenyl (for $L^{22}F$) is halved. Steric hindrance due to an overlap of the van der Waals forces of MTX and the phenylalanine would presumably raise the energy of interaction and weaken ligand binding. This would be even greater for the hydroxyphenyl of tyrosine, and therefore this mutant was anticipated to display the most diminished MTX binding.

Predictions pertaining to APT required the assumption that the pteridine and pteridine C_6 substituent adopt a similar conformation to the analogous portions of MTX. On this basis and noting that this compound lacks the N_{10} methyl, it was predicted that this compound would have greater affinity (than MTX) for the mutants with bulky side-chain replacements ($L^{22}F$ and $L^{22}Y$).

All species of position 22 mutant DHFR displayed good stability when in crude form, which is consistent with little disruption of protein tertiary structure. With a few exceptions, the experimentally derived kinetic parameters have agreed well with the modeling predictions. Values of k_{cat} and K_m ^{H_2}folate obtained for WT agree with those reported previously (14, 27) under similar conditions of pH and temperature. The K_m values for 7,8-dihydrofolate for mutant species (Table 2) are all elevated, although only ~2-fold for those involving bulkier side-chain replacements of phenylalanine and Y. Decreased affinity for 7,8-dihydrofolate in this series is, however, less dramatic than that found for the murine enzymes. The K_m value for $L^{22}F$ (0.16 μM) is 3.4-fold lower than its murine counterpart [0.54 μM, CHO (30)], suggesting that the human version of this mutant would function as a better catalyst *in vivo*.

At neutral pH (pH 7.4, MATS assay buffer), the catalytic potential (k_{cat}) is more affected by phenylalanine and tyrosine replacements than by the more conserved side-chain replacements ($L^{22}I$ and $L^{22}M$), which are nearly identical to WT. An explanation for this finding is that the former mutants have become partially ($L^{22}F$) or completely ($L^{22}Y$) rate limited by a step other than dissociation of 5,6,7,8-tetrahydrofolate (31, 32). This is undoubtedly due to a nonoptimal alignment of substrate for protonation and/or hydride transfer with the bulkier substitutions. $L^{22}F$ and $L^{22}Y$, even at the most acidic pH tested, also do not display a k_{cat} comparable to or surpassing WT. This implies that neither mutant has an increased rate of product release, which is observed when WT of enzyme is exposed to chaotropic agents, or for specific amino acid replacements that affect catalysis via more global changes in DHFR tertiary structure (7). Also, the lack of any noticeable differences in the reaction progress curves for each of the DHFR species when either 7,8-dihydrofolate or NADPH was present as the limiting reagent indicates a lack of any dramatic effect on product affinity (relative to substrate) for DHFR variants.

Although the K_m values for substrate affinity for mutants is severalfold reduced, the binding affinity for MTX is more dramatically affected, particularly for $L^{22}F$ and $L^{22}Y$, and as predicted from modeling. Presumably, the far greater reduced binding observed for $L^{22}Y$ (1600-fold) compared with $L^{22}F$ (88-fold) is due to a greater steric disruption by the hydroxy-benzoyl group, which is oriented toward the bridge region of the inhibitor (Fig. 3b). For the more conserved side-chain replacements ($L^{22}I$ and $L^{22}M$), the binding of antifolates tested are affected only marginally.

The finding that APT binding is reduced to an extent comparable to that for MTX was contrary to our predictions from modeling. This implies that the C_6—C_9—N_{10} bridge, and not the N_{10}-methyl group alone, is involved in the steric hindrance by substituted phenylalanine and tyrosine residues. Alternatively, the positioning of APT in the active site may be different than that of MTX. No crystal structures for APT in a complex with any eukaryotic or prokaryotic species of DHFR have been reported.

The finding that $L^{22}F$ is potently inhibited by PTX was surprising. We tested the sensitivity of the CHO cell line harboring $L^{22}F$ mutant DHFR to PTX and other antifolates. The cell culture cytotoxicity data for this CHO cell line ($L^{22}F$) agreed with the inhibition data obtained from enzyme kinetic studies (Tables 3 and 4). This mutant (for both human and CHO) may retain avid binding of PTX due to the methoxyphenyl group of inhibitor orienting differently in the active site relative to that for TMTX and relative to the *p*-aminobenzoyl group of APT and MTX, as recently described from an analysis of crystal structure data (unrefined) for PTX in ternary complex with human DHFR and cofactor (33). In this structure, the dimethoxyphenyl of PTX is approximately perpendicular to the plane of the 5-deazapteridine ring but, more importantly, sits on the opposite side of the plane (i.e., points in the opposite direction) to that of the *p*-aminobenzoyl group of either folic acid or MTX (see Fig. 1b for structures). The binding of PTX resembles that for trimethoprim complexed with bacterial DHFR, which has its trimethoxyphenyl group positioned "low" (24) in the active site pocket pointing toward the cofactor (34). This positioning of PTX, possibly due to the shortened bridge region, results in a greater distance between drug and residue 22. The crystal structure of

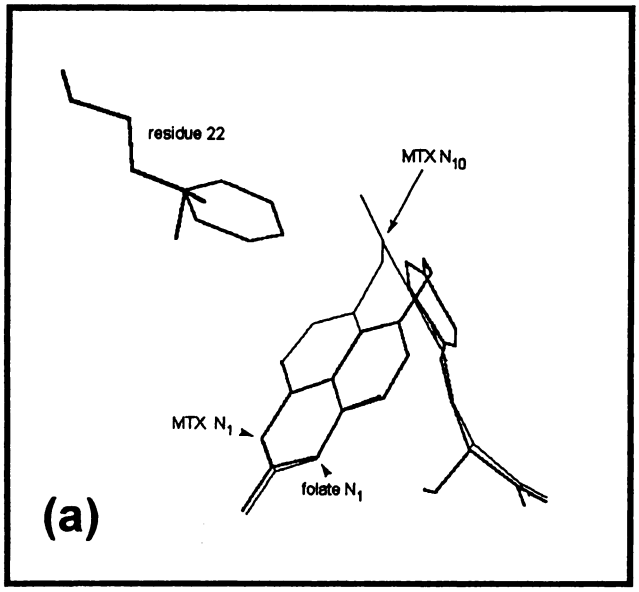

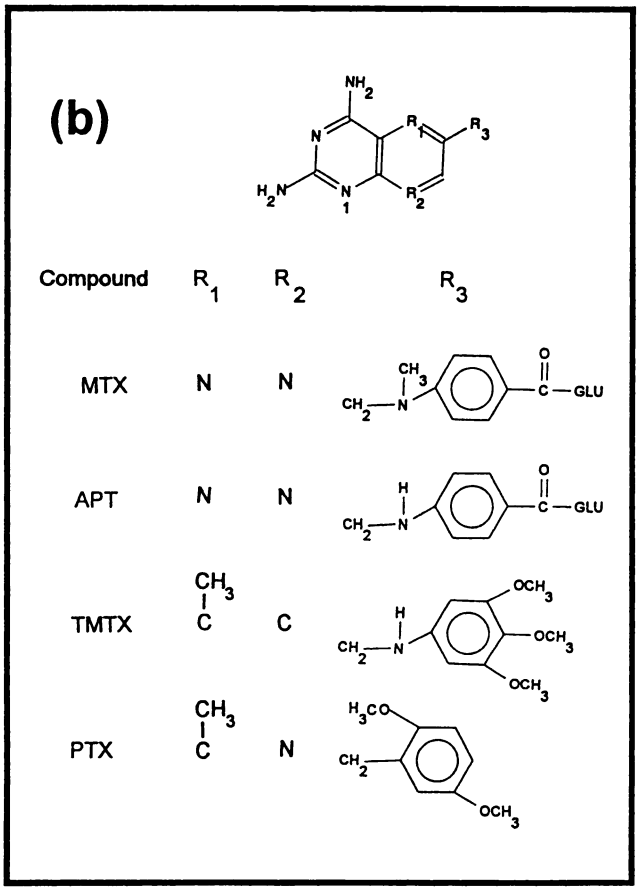

Fig. 3. Human DHFR active site model. a, Positioning of Leu-22 of WT and superimposed phenyl residue in relation to folic acid (*thick lines*) and MTX (*thin lines*). The benzoyl group of both ligands are close to perpendicular to the plane of the page; the N_{10} methyl of MTX projects behind the plane. b, Chemical structures of antifolates (*GLU*, glutamyl residue).

TMTX complexed with an active site mutant of human DHFR ($F^{31}A$) indicates that the trimethoxyl group is oriented in a similar direction to folate or MTX (33). This would explain the similar reduced binding for this antifol for $L^{22}F$ as found for MTX and APT.

Inspection of the inhibition progress curves also reveals that the mechanism of inhibition or at least the pathway to formation of a final tight antifolate complex with MTX, as usually observed for all WT species of DHFR, is impaired for $L^{22}F$ and $L^{22}Y$. For the latter, an initial inhibited reaction rate is seen but without slow onset of further inhibition or "isomerization" for all antifolates tested (data not presented). A similar lack of isomerization has previously been noted for the mouse $G^{15}W$ (7) and for a human active site mutant, $F^{31}G$ (32). Although the molecular basis for the isomerization remains unknown, it appears that it must not be essential for catalysis as many of these mutant species have reasonable catalytic efficiency (k_{cat}/K_m), even at physiological pH. The proposal (35) that the inhibition isomerization is implicitly associated with the reorientation of the active site Phe-31 residue may be the basis for what is observed for the current set of mutants; however, this proposition is difficult to rationalize with the facts that the $G^{15}W$ mouse mutant also does not display isomerization (in combination with MTX) (7) and that this amino acid substitution is 10–15 Å from the active site. Regardless of the precise molecular basis, the lack of isomerization reported here for some of the mutant/antifolate combinations contributes to a significant portion of lost binding energy; for MTX inhibition of WT human DHFR, this isomerization enhances binding 60-fold (35). Interestingly, an isomerization was detectable for $L^{22}F$ inhibition by PTX, which suggests that the proposed conformational change is not completely lost for this mutant, but rather that antifolates (particularly MTX, APT, and TMTX) do not strongly stabilize the conformationally altered state.

The identification of possible residue-22 mutants for use as dominant selectable markers in gene transfer or as a means to impart antifolate resistance to bone marrow progenitor cells has been another important aspect of this study. Clearly, $L^{22}F$ and $L^{22}Y$ seem to be the most promising of the species reported here due to their markedly diminished antifolate binding. A direct quantitative comparison of mutants is difficult, however, as the relative importance of each individual desirable attribute (i.e., high K_i, k_{cat}, low K_m, and good stability) in providing *in vivo* resistance has yet to be determined. Nevertheless, the values of $K_i \cdot k_{cat}/K_m$ as used by Blakley *et al.* (27, 32) may provide a general comparative index, although without regard to intrinsic stability of the protein. Under the conditions used in this study, these values (expressed as $sec^{-1} \times 10^3$) for $L^{22}I$, $L^{22}M$, $L^{22}F$, and $L^{22}Y$ (with respect to MTX) are 0.04, 0.16, 4.90, and 19.80, respectively. The latter two mutants are superior to WT ($K_i \cdot k_{cat}/K_m$ = 0.20) and comparable to the three best human phenylalanine mutants of DHFR, i.e., $F^{31}S$, $F^{31}A$, and $F^{31}G$ as reported recently (32), which have values of 3.82, 7.95, and 8.97, respectively. Previous experience in this laboratory has, however, indicated that although the expression vector used and the mode of transfection are important, the actual amount of DHFR expressed after gene transfection is generally low (12). For this reason, the human $L^{22}Y$ mutant, while having the highest value of $K_i \cdot k_{cat}/K_m$, has the lowest catalytic potential even at saturating substrate conditions and therefore may not be greatly superior to $L^{22}F$ or the Phe-31 mutants. The human $L^{22}F$ should be superior to the rodent versions of this mutant, which have been used by a number of laboratories to confer MTX resistance to several cell lines (36, 37).

Resistance to the antimalarial DHFR inhibitor, pyrimethamine, has been ascribed almost exclusively to the evolution of altered DHFRs in *Plasmodium falciparum* (38). To date, in limited clinical studies, mutations in DHFR have not been detected (39). The finding that $L^{22}F$ is potently inhibited by PTX indicates that a search for inhibitors of mutant versions of plasmodium DHFR and human DHFR, if this is a mechanism of resistance to MTX in human tumors, is a worthwhile goal.

Note Added in Proof

During preparation of this article, Lewis *et al.* (40) arrived at similar conclusions regarding substitutions at position 22 of human DHFR.

References

1. Srimatkandada S., B. I. Schweitzer, B. A. Moroson, S. Dube, and J. R. Bertino. Amplification of a polymorphic dihydrofolate reductase gene expressing an enzyme with decreased binding to methotrexate in a human colon carcinoma cell line, HCT-8R4, resistant to this drug. *J. Biol. Chem.* **264:**3524–3528 (1989).
2. Simonsen, C. C., and A. D. Levinson. Isolation and expression of an altered mouse dihydrofolate reductase cDNA. *Proc. Natl. Acad. Sci. USA* **80:**2495–2499 (1983).
3. Melera, P. W., J. P. Davide, C. A. Hession, and K. W. Scotto. Phenotypic expression in *Escherichia coli* and nucleotide sequence of two Chinese hamster lung cell cDNAs encoding two different dihydrofolate reductases. *Mol. Cell. Biol.* **4:**38–48 (1984).
4. Dicker, A. P., M. Volkenandt, B. I. Schweitzer, D. Banerjee, and J. R. Bertino. Identification and characterization of a gene from the methotrexate-resistant Chinese hamster ovary cell line Pro-3 MTXRIII. *J. Biol. Chem.* **265:**8317–8321 (1990).
5. McIvor, R. S., and C. C. Simonsen. Isolation and characterization of a variant dihydrofolate reductase cDNA from methotrexate-resistant murine L5178Y cells. *Nucleic Acids Res.* **18:**7025–7032 (1990).
6. Yu, M., and P. W. Melera. Allelic variation in the dihydrofolate reductase gene at amino acid position 95 contributes to antifolate resistance in Chinese hamster cells. *Cancer Res.* **53:**6031–6035 (1993).
7. Dicker, A. P., M. C. Waltham, M. Volkenandt, B. I. Schweitzer, G. M. Otter, F. A. Schmid, F. M. Sirotnak, and J. R. Bertino. Methotrexate resistance in an *in vivo* mouse tumor due to a non-active dihydrofolate reductase mutation. *Proc. Natl. Acad. Sci. USA* **90:**11797–11801 (1993).
8. Flintoff, W. F., and K. Essani. Methotrexate-resistant Chinese hamster ovary cells contain a dihydrofolate reductase with an altered affinity for methotrexate. *Biochemistry* **19:**4321–4327 (1980).
9. Flintoff, W. F., S. V. Davidson, and L. Siminovitch. Isolation and partial characterization of three methotrexate-resistant phenotypes from Chinese hamster ovary cells. *Somatic Cell Genet.* **2:**245–261 (1976).
10. Bertino, J. R. 'Turning the tables': making normal marrow resistant to chemotherapy (editorial). *J. Natl. Cancer Inst.* **82:**1234–1235 (1990).
11. Corey, C. A., A. Desilva, C. Holland, and D. A. Williams. Serial transplantation of methotrexate-resistant bone marrow protection of murine recipients from drug cytotoxicity by progeny of transduced stem cells. *Blood* **75:**337–343 (1990).
12. Li, M.-X., D. Banerjee, S.-C. Zhao, B. I. Schweitzer, S. Mineishi, E. Gilboa, and J. R. Bertino. Development of a retroviral construct containing a human mutated dihydrofolate reductase cDNA for hematopoietic stem cell transduction. *Blood* **83:**3403–3408 (1994).
13. Williams, D. A., K. Hsieh, A. Desilva, and R. C. Mulligan. Protection of bone marrow transplant recipients from lethal doses of methotrexate-resistant bone marrow. *J. Exp. Med.* **166:**210–218 (1987).
14. Schweitzer, B. I., S. Srimatkandada, H. Gritsman, R. Sheridan, R. Venkataraghavan, and J. R. Bertino. Probing the role of two hydrophobic active site residues in the human dihydrofolate reductase by site directed mutagenesis. *J. Biol. Chem.* **264:**20786–20795 (1989).
15. Higuchi, R., B. Krummel, and R. K. Saiki. A general method of *in vitro* preparation and specific mutagenesis of cDNA fragments: study of protein and DNA interaction. *Nucleic Acids Res.* **16:**7351–7367 (1988).
16. Sanger, F., S. Nicklen, and A. R. Coulson. DNA sequencing with chain terminating inhibitors. *Proc. Natl. Acad. Sci. USA* **74:**5463–5467 (1977).
17. Hillcoat, B. L., P. F. Nixon, and R. L. Blakley. Effect of substrate decomposition on the spectrophotometric assay of dihydrofolate reductase. *Anal. Biochem.* **21:**178–189 (1967).
18. Ellis, K. J., and J. F. Morrison. Buffers of constant ionic strength for studying pH dependent processes. *Methods Enzymol.* **87:**405–426 (1982).
19. Dunn, S. M. J., and R. W. King. Kinetic of ternary complex formation between dihydrofolate reductase, coenzyme and inhibitor. *Biochemistry* **19:**766–733 (1980).
20. Bradford, M. A rapid and sensitive method for the quantitation of microgram quantities of protein utilizing the principle of protein-dye binding. *Anal. Biochem.* **21:**178–189 (1976).
21. Duggleby, R. G. Regression analysis of nonlinear Arrhenius plots: an empirical model and a computer program. *Comput. Biol. Med.* **14:**447–455 (1984).
22. Williams, J. W., J. F. Morrison, and R. G. Duggleby. Methotrexate, a high affinity pseudosubstrate of dihydrofolate reductase. *Biochemistry* **18:**2567–2573 (1979).
23. Williams, J. W., and J. F. Morrison. The kinetics of reversible tight binding inhibition. *Methods Enzymol.* **63:**437–467 (1979).
24. Matthews, D. A., J. T. Bolin, J. M. Burridge, D. J. Filman, K. W. Volz, B. T. Kaufman, C. R. Beddell, J. N. Champness, D. K. Stammers, and J. Kraut. Dihydrofolate reductase: the stereochemistry of inhibitor selectivity. *J. Biol. Chem.* **260:**381–391 (1985).
25. Oefner, C., A. D'Arcy, and F. K. Winkler. Crystal structure of human dihydrofolate reductase complexed with folate. *Eur. J. Biochem.* **174:**377–385 (1988).
26. Appleman, J. R., W. A. Beard, T. J. Delcamp, N. J. Prendergast, J. H. Freisheim, and R. L. Blakley. Unusual transient- and steady-state behavior is predicted by the kinetic scheme operational for recombinant human dihydrofolate reductase. *J. Biol. Chem.* **265:**2740–2748 (1990).
27. Nakano, T., H. T. Spencer, J. R. Appleman, and R. L. Blakley. Critical role of phenylalanine 34 of human dihydrofolate reductase in substrate and inhibitor binding and in catalysis. *Biochemistry* **33:**9945–9952 (1994).
28. Flintoff, W. F., M. K. Weber, C. R. Nagainis, A. K. Essani, D. Robertson, and W. Salser. Overproduction of dihydrofolate reductase and gene amplification in methotrexate-resistant Chinese hamster ovary cells. *Mol. Cell. Biol.* **2:**275–285 (1982).
29. Davies, J. F., T. J. Delcamp, N. J. Prendergast, V. A. Ashford, J. H. Freisheim, and J. Kraut. Crystal structures of recombinant human dihydrofolate reductase complexed with folate and 5-deazafolate. *Biochemistry* **29:**9467–9479 (1990).
30. Schweitzer, B. I., H. Gritsman, A. P. Dicker, M. Volkenandt, and J. R. Bertino. Mutations at hydrophobic residues in dihydrofolate reductase, in *Chemistry and Biology of Pteridines: Pteridines and Folic Acid Derivatives* (H.-C. Curtis, S. Ghisla, and N. Blau, eds.). de Gruyter, Berlin, 760–764 (1990).
31. Beard, W. A., J. R. Appleman, T. J. Delcamp, J. H. Freisheim, and R. L. Blakley. Hydride transfer by dihydrofolate reductase: causes and sequences of the wide range of rates exhibited by bacterial and vertebrate enzymes. *J. Biol. Chem.* **264:**9391–9399 (1989).
32. Chunduru, S. K., V. Cody, J. R. Luft, W. Pangborn, J. R. Appleman, and R. L. Blakley. Methotrexate-resistant variants of human dihydrofolate reductase. *J. Biol. Chem.* **269:**9547–9555 (1994).
33. Cody, V., A. Wojtczak, T. I. Kalman, J. H. Freisheim, and R. L. Blakley. Conformational analysis of human dihydrofolate reductase inhibitor complexes: crystal structure determination of wild type and F31 mutant binary and ternary complexes, in *Chemistry and Biology of Pteridines and Folates: Pteridines and Folic Acid Derivatives* (J. E. Ayling, M. G. Nair, and C. M. Baugh, eds.). Plenum Press, New York, 1481–1486 (1993).
34. Schweitzer, B. I., A. P. Dicker, and J. R. Bertino. Dihydrofolate reductase as a therapeutic target. *FASEB J.* **4:**2441–2452 (1990).
35. Appleman, J. R., N. Prendergast, T. J. Delcamp, J. H. Freisheim, and R. L. Blakley. Kinetics of the formation and isomerization of methotrexate complexes of recombinant human dihydrofolate reductase. *J. Biol. Chem.* **263:**10304–10313 (1988).
36. Hussain, A., D. Lewis, M. Yu, and P. W. Melera. Construction of a dominant selectable marker using a novel dihydrofolate reductase. *Gene* **112:**179–188 (1992).
37. Morris, J. A., and R. S. McIvor. Saturation mutagenesis at dihydrofolate reductase codons 22 and 31. *Biochem. Pharmacol.* **47:**1207–1220 (1994).
38. Hyde, J. E. The dihydrofolate reductase-thymidylate synthase gene in the drug resistance malaria parasites. *Pharmacol. Ther.* **48:**45–59 (1990).
39. Bertino, J. R., A. Romanini, A. P. Dicker, M. Volkenant, J. T. Lin, and B. I. Schweitzer. Resistance to methotrexate in experimental models and in patients, in *Chemistry and Biology of Pteridines: Pteridines and Folic Acid Derivatives* (H.-C. Curtis, S. Ghisla, and N. Blau, eds.). de Gruyter, Berlin, 1089–1099 (1990).
40. Lewis S. W., V. Cody, N. Galitsky, J. R. Luft, W. Pangborn, S. K. Chunduru, H. T. Spencer, J. R. Appleman, and R. L. Blakley. Methotrexate-resistant variants of human dihydrofolate reductase with substitutions of leucine 22. *J. Biol. Chem.* **270:**5057–5064 (1995).

Send reprint requests to: Dr. Joseph R. Bertino, Memorial Sloan-Kettering Cancer Center, 1275 York Avenue, Box 78, New York, NY 10021. E-mail: j-bertino@mskcc.org